Analytical Biochemistry 445 (2014) 24–29

Contents lists available at ScienceDirect

Analytical Biochemistry

journal homepage: www.elsevier.com/locate/yabio

A mediator-free glucose biosensor based on glucose oxidase/chitosan/α-zirconium phosphate ternary biocomposite

Li-Min Liu *, Jiwu Wen, Lijun Liu, Deyong He, Ren-yun Kuang, Taqing Shi

School of Chemistry and Chemical Engineering, Key Laboratory of Coordination Chemistry of Jiangxi Province, Institute of Applied Chemistry, Jinggangshan University, Ji'an, Jiangxi 343009, China

ARTICLE INFO

Article history:
Received 12 July 2013
Received in revised form 27 September 2013
Accepted 4 October 2013
Available online 14 October 2013

Keywords:
Glucose oxidase
α-Zirconium phosphate
Co-intercalation
Biosensor
Direct electron transfer

ABSTRACT

A novel glucose oxidase/chitosan/α-zirconium phosphate (GOD/chitosan/α-ZrP) ternary biocomposite was prepared by co-intercalating glucose oxidase (GOD) and chitosan into the interlayers of α-zirconium phosphate (α-ZrP) via a delamination–reassembly procedure. The results of X-ray diffraction, infrared spectroscopy, circular dichroism, and ultraviolet spectrum characterizations indicated not only the layered and hybrid structure of the GOD/chitosan/α-ZrP ternary biocomposite but also the recovered activity of the intercalated GOD improved by the co-intercalated chitosan. By depositing the GOD/chitosan/α-ZrP biocomposite film onto a glassy carbon electrode, the direct electrochemistry of the intercalated GOD was achieved with a fast electron transfer rate constant, k_s, of 7.48 ± 3.52 s^{-1}. Moreover, this GOD/chitosan/α-ZrP biocomposite modified electrode exhibited a sensitive response to glucose in the linear range of 0.25–8.0 mM (R = 0.9994, n = 14), with a determination limit of 0.076 mM.

Over the past two decades, the functional biocomposites formed by intercalating of biomolecules into the interlayers of layered inorganic solids have attracted special attention. First, the expandable interlayer space of layered materials is suitable for accommodating different-sized biomolecules [1]. Second, the high thermal stability of inorganic materials is advantageous for protecting the entrapped biomolecules from the environmental disturbances [2,3]. Third, the good biocompatibility of inorganic materials is considerably favorable for maintaining the activity of incorporated biomolecules [4,5]. So, this kind of bioinorganic hybrids displays the potential applications in biomimic engineering [6,7], drug delivery [8,9], and biocatalytic system [10,11].

On the other hand, the direct electron transfer of electroactive biomolecules on solid electrode has attracted more and more attention recently because the third-generation biosensors can overcome the drawbacks of high applied potential and various interfering reactions [12,13]. However, it is difficult for the roteins to exchange electrons directly with the bare solid electrodes. One of the reasons is the deep burying of the electroactive center by a protein's shell, which causes a long distance between the redox center of protein and the electrode surface [14,15]. To achieve the direct electron transfer between the redox proteins and the based electrode, biomembrane-like materials [16,17], polymers [18,19], sol–gel [20,21], and inorganic nanoparticles [22–25] acting as matrices to immobilize protein were investigated. Recently, some biocomposites formed by intercalating the redox proteins into the layered inorganic materials demonstrated the direct electrochemical performance on solid electrodes, suggesting that it is a simple but efficient strategy to construct the third-generation biosensors [26–29].

Compared with the intercalation of a single type of biomolecule into the layered solids [1–11,26–29], the co-immobilization of multiple components into the layered clay demonstrated the advantages to improving the performance of resulting composites. For example, the co-intercalated DNA enhanced the activity of protein immobilized in an α-zirconium phosphate (α-ZrP)[1] matrix [30], and the co-intercalated polymer exhibited significant influence on the drug release from aminopropyl-functionalized magnesium phyllosilicate [31]. We have also reported a DNA/chitosan/α-ZrP ternary composite in which the co-intercalated chitosan acted as an intermediary to modulate the reversible immobilization and release of DNA from the interlayers of α-ZrP [32].

In this work, the synergistic effect of co-intercalated glucose oxidase (GOD) and chitosan on the electrochemical performance of GOD/chitosan/α-ZrP ternary composite modified electrode was investigated in order to obtain a novel mediator-free biosensor. GOD has been widely used in glucose biosensor construction for monitoring the glucose levels in diabetics [33], but the direct

* Corresponding author. Fax: +86 796 8110665.
E-mail address: llm24@126.com (L.-M. Liu).

[1] *Abbreviations used:* α-ZrP, α-zirconium phosphate; GOD, glucose oxidase; pI, isoelectric point; HAc, acetic acid; GCE, glassy carbon electrode; TBAOH, tetrabutylammonium hydroxide; XRD, X-ray diffraction; FTIR, Fourier transform infrared; IR, infrared; CD, circular dichroism; UV, ultraviolet–visible; SCE, saturated calomel electrode; CV, cyclic voltammogram; E_p, peak potential.

0003-2697/$ - see front matter © 2013 Elsevier Inc. All rights reserved.
http://dx.doi.org/10.1016/j.ab.2013.10.005

electron transfer between GOD and the based electrode cannot be achieved easily because of the rigid structure and the larger molecular weight (152,000–186,000 Da) of GOD. As confirmed by previous works, the nanomaterial films such as gold colloidal [34], carbon nanotubes [35], and mesoporous silica [36] were good promoters for the direct electrochemistry of GOD. However, the direct electron transfer of GOD intercalated into layered α-ZrP has not been reported. Considering the isoelectric point (p*I*) 4.9 of GOD and the pK_a 6.3 of chitosan, the reassembly of GOD, chitosan, and exfoliated α-ZrP nanosheets was operated in a 0.1% acetic acid (HAc) buffer solution with a pH of 5.5. On this pH, the positive charged chitosan and the negative charged GOD were co-intercalated successfully into the interlayers of α-ZrP, producing the GOD/chitosan/α-ZrP ternary composite with an inorganic–organic hybrid structure. The fast and direct electron transfer of the intercalated GOD was achieved by depositing the GOD/chitosan/α-ZrP composite film onto a glassy carbon electrode (GCE). Moreover, this GOD/chitosan/α-ZrP ternary composite modified electrode exhibited an enhanced response to glucose larger than that of corresponding GOD/α-ZrP binary composite modified electrode because of the presence of the co-intercalated chitosan (Scheme 1).

Materials and methods

Materials

GOD was purchased from Sigma Chemical. Chitosan (deacetylation) was obtained from Nanjing Debao Biochemical Equipment. Tetrabutylammonium hydroxide (TBAOH) aqueous solution (10 wt%) was purchased from Shanghai Chemical Reagent. The human serum sample was offered by Ji'an Central Hospital. All other reagents were of analytical grade, and the water used in the experiments was deionized.

Synthesis and delamination of α-ZrP

The α-ZrP was prepared according to the procedure as follows. First, 4.79 g of phosphoric acid in 75 ml of water was added to 75 ml of $ZrOCl_2$ solution containing 2.42 g of $ZrOCl_2{\cdot}8H_2O$ under stirring dropwise. Then, the mixture was heated and kept at 90 °C for 48 h. The white solid obtained via centrifuging was washed with deionized water and acetone, respectively. The α-ZrP solid was then dried overnight at 60 °C.

The delamination of α-ZrP was performed by sonicating 5 ml of aqueous suspension containing α-ZrP (0.1 g) and TBAOH (0.17 g) for 1 h. The final concentration of the exfoliated α-ZrP was approximately 20 mg ml^{-1}.

Preparation of GOD/chitosan/α-ZrP and GOD/α-ZrP composites

First, 30 μl of 5.0 mg ml^{-1} GOD stock solution (0.1% HAc, pH 5.5), 90 μl of 2.0 mg ml^{-1} chitosan (0.1% HAc, pH 5.5), and 30 μl of 20 mg ml^{-1} exfoliated α-ZrP suspension were added into 2.85 ml of 0.1% HAc buffer solution (pH 5.5) with shaking in sequence. After equilibrating for 24 h at room temperature, the sample was separated by centrifugation and the precipitate was washed by 0.1% HAc buffer (pH 5.5) twice. Then, the solid was lyophilized for X-ray diffraction (XRD) and Fourier transform infrared (FTIR) studies. For preparing the GOD/chitosan/α-ZrP modified electrode, the lyophilized solid was dispersed thoroughly in 100 μl of 0.1% HAc (pH 5.5) again.

Construction of biosensors

GCEs that were 3 mm in diameter were sequentially polished with 1, 0.3, and 0.05 μm alumina powder, followed by sonication in acetone and then doubly distilled water. Then, the electrodes were dried under a stream of nitrogen gas. The prepared GOD/chitosan/α-ZrP suspension was shaken for 5 min before use, and then 5 μl of the mixture was dropped onto the surface of a GCE and dried at room temperature.

Measurements

Powder XRD patterns were collected on a Philips X'pert X-ray diffractometer. Infrared (IR) spectroscopy measurements were recorded on a Bruker Fourier transform spectrometer (Vector 22). Circular dichroism (CD) spectra were detected on a Jasco 810 spectropolarimeter. Ultraviolet–visible (UV) absorption spectra were measured with a PerkinElmer Lambda 35 spectrophotometer.

Electrochemical measurements were conducted on a CHI660B workstation (Shanghai Chenhua). All electrochemical experiments were performed with a conventional three-electrode system using a saturated calomel electrode (SCE) as the reference, a platinum wire as the counter electrode, and the modified GCE as the working electrode. Buffer solutions were purged with highly purified nitrogen for 30 min before the electrochemical experiments, and a nitrogen environment was maintained in the cell by continuously bubbling N_2 during the course of the experiments.

Results and discussion

Characterization of GOD/chitosan/α-ZrP composite

The FTIR and UV absorption spectra confirmed the formation of the GOD/chitosan/α-ZrP ternary composite. After both GOD and chitosan were incubated with the exfoliated α-ZrP in a 0.1% HAc buffer solution at pH 5.5, the flocculent precipitates were produced. As shown in Fig. 1, the FTIR spectra of these lyophilized precipitates display all of the characteristic absorbance bands of GOD, chitosan, and α-ZrP. The absorbance band at 1541 cm^{-1} comes from the stretch of the polypeptide amide II of the intercalated GOD. The band at 1639 cm^{-1} is attributed to both the polypeptide amide I stretch of the intercalated GOD and the carbonyl vibration

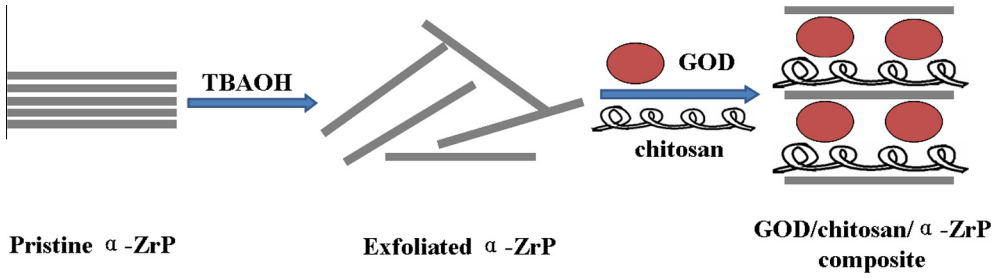

Scheme 1. GOD and chitosan co-intercalated into α-ZrP to form the GOD/chitosan/α-ZrP ternary composite. TBAOH, tetrabutylammonium hydroxide.

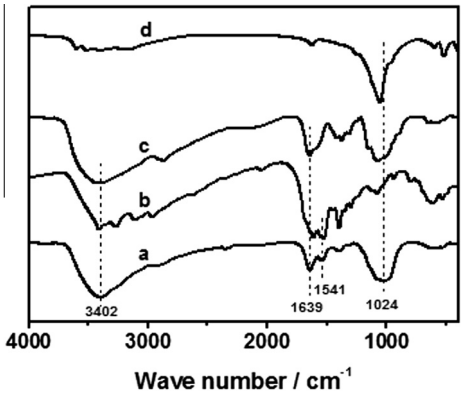

Fig.1. FTIR spectrograms of GOD/chitosan/α-ZrP composite (a), native GOD (b), native chitosan (c), and α-ZrP (d).

of the intercalated chitosan. Compared with that of the native GOD, the slight shift of polypeptide amide II stretch from 1530 to 1541 cm^{-1} suggests the electrostatic interaction among GOD, chitosan, and α-ZrP. The broad band from 3700 to 3000 cm^{-1} should be attributed to the vibrations of both N-H and O-H in the co-intercalated GOD and chitosan. The hydrogen bonding and the electrostatic interaction among the intercalated GOD, chitosan, and α-ZrP may be the origin for the minor deviation from the bands of the native GOD and chitosan. Moreover, the intense and broad band from 1280 to 850 cm^{-1} can be primarily attributed to the vibration of P-O in the α-ZrP.

The XRD pattern of the GOD/chitosan/α-ZrP ternary composite shown in Fig. 2 demonstrates that the layered structure of α-ZrP is considerably retainable after the delamination and reassembly procedures. The interlayer distance of pristine α-ZrP is 0.76 nm, calculated according to the diffraction peak at 2θ of 11.749° shown in the inset of Fig. 2. As for the GOD/chitosan/α-ZrP ternary composite, a new diffraction peak at lower angle range was observed at 2θ of 0.835°, indicating that the interlayer distance of the ternary hybrid is 10.57 nm. Moreover, the diffraction peak at 2θ of 11.749 disappeared for the GOD/chitosan/α-ZrP ternary composite. The increase of the interlayer distance from pristine α-ZrP is 9.81 nm, which is larger than both the dimensions (3.7 × 5.2 × 6.0 nm) of a GOD molecule [37] and the thickness (0.38 nm) of a chitosan monolayer [38], indicating that GOD and chitosan were co-intercalated successfully into the interlayer galleries of α-ZrP.

The possible change in protein conformation after both GOD and chitosan bound with α-ZrP was monitored by CD spectra. In Fig. 3, the native GOD exhibits the strong negative bands at 207 and 218 nm that are characteristic of the α-helical structure of protein. After GOD was bound with α-ZrP to form the GOD/α-ZrP binary composite, the intensities of the dual bands decreased remarkably. This result indicated that the protein secondary structure was influenced to a large extent after GOD was combined with α-ZrP alone. However, in the GOD/chitosan/α-ZrP ternary composite, the intensities of the dual bands are almost comparable to that of native GOD, with only the wavelengths shifting slightly to 213 and 219 nm, respectively. These results suggested that the protein secondary structure of the entrapped GOD in the interlayers of α-ZrP was recovered, attributed to the presence of the co-intercalated chitosan.

The results of UV characterization further confirmed that the secondary structure of the intercalated protein can be recovered through co-intercalating GOD and chitosan into the interlayer galleries of α-ZrP. As shown in Fig. S1 of the online supplementary material, the characteristic band of native GOD is located at 274 nm. After GOD was combined with α-ZrP alone, not only was the absorbance intensity obviously weakened but also the characteristic wavelength of the incorporated GOD in the GOD/α-ZrP binary composite was almost unidentifiable. However, in the case of both GOD and chitosan reacted with α-ZrP, the characteristic wavelength of intercalated GOD in the GOD/chitosan/α-ZrP ternary composite is almost unchanged compared with that of the native GOD, with only the absorbance intensity being slightly weakened.

Direct electrochemistry of GOD/chitosan/α-ZrP modified electrode

Fig. 4 shows the cyclic voltammograms (CVs) of GOD/chitosan/α-ZrP composite electrode in a 0.1% HAc buffer solution at pH 5.5. A couple of reversible and well-defined redox peaks at −370 and −408 mV were observed, with an apparent formal peak potential (E_p) of −389 mV and a peak-to-peak separation (ΔE_p) of 38 mV at a scan rate of 100 mV s^{-1}. The results clearly demonstrated that the GOD direct electrochemistry was achieved by co-intercalating GOD and chitosan into the interlayer galleries of α-ZrP.

The effect of the scan rate on the response of the GOD/chitosan/α-ZrP electrode is shown in Fig. 5. With the increase of scan rate from 0.1 to 1.0 V s^{-1}, both the reduction and oxidation peak currents (I_p) increased linearly, suggesting a surface-controlled process. The small peak-to-peak separation indicated a fast electron transfer rate. According to Laviron's theory [39], when the peak-to-peak separation is less than 200 mV, the electron transfer rate constant, k_s, can be estimated according to the formula $k_s = mnFv/RT$, where m is a parameter related to the peak-to-peak separation, n is the number of transferred electrons, F is the

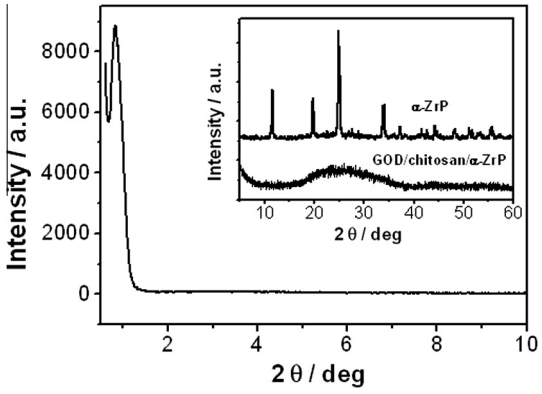

Fig.2. Powder XRD diffraction spectrograms of GOD/chitosan/α-ZrP composite and pristine α-ZrP (inset).

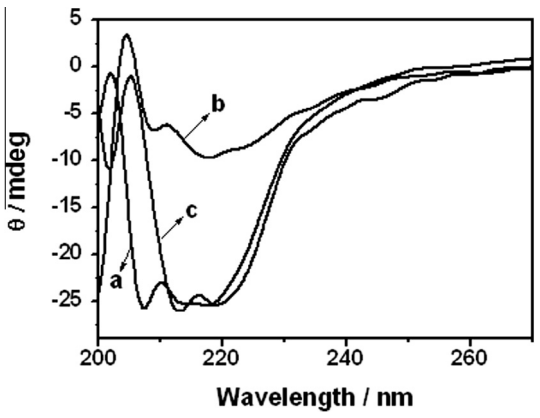

Fig.3. CD spectrograms of native GOD (a), GOD/α-ZrP (b), and GOD/chitosan/α-ZrP (c) composite.

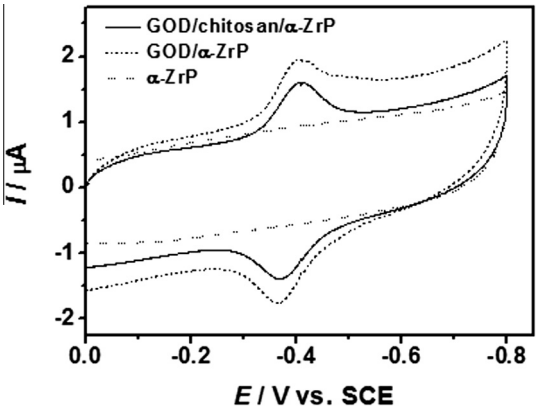

Fig.4. CVs of pre-exfoliated α-ZrP, GOD/α-ZrP, and GOD/chitosan/α-ZrP composite modified electrode in 0.1% HAc buffer solution (pH 5.5) at a scan rate of 100 mV s^{-1}.

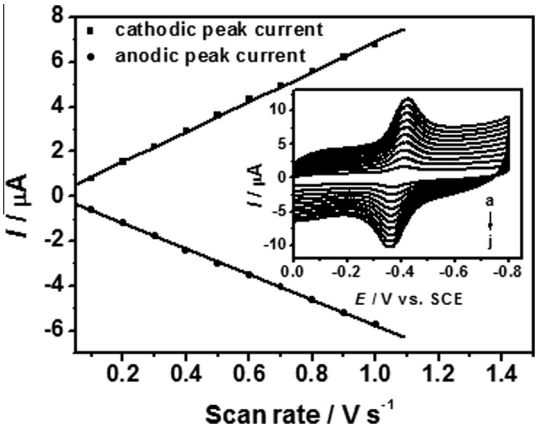

Fig.5. Plots of cathodic and anodic peak current versus scan rate and CVs (inset) of GOD/chitosan/α-ZrP composite modified electrode at scan rates from 0.1 to 1.0 V s^{-1} in 0.1% HAc buffer solution at pH 5.5.

Faraday's constant, v is the scan rate, R is the universal gas constant, and T is the temperature. The peak-to-peak separations were 38, 40, 43, and 48 mV at 100, 200, 300, and 400 mV s^{-1}, respectively. The average k_s value was calculated to be 7.37 ± 3.9 s^{-1}, which is similar to that of GOD immobilized on carbon nanotubes/chitosan matrix [35] and manganese oxide/polymer composite film [40] but larger than the value of GOD incorporated into gold nanoparticles/carbon nanotubes composite film [41] and GOD assembled in the zinc oxide nanoparticles/carbon nanotubes multilayers structure [42].

The direct electrochemistry of the GOD/chitosan/α-ZrP composite exhibited a strong dependence on the medium pH. The increase of pH caused a negative shift for the reduction and oxidation peaks, as shown in Fig. S2 of the supplementary material. Furthermore, all changes in peak potentials with pH were reversible. In the range of pH values from 4.0 to 9.0, the relationship between the apparent formal peak potential (E_p) and pH was linear with a slope of −57 mV pH^{-1}. This value was close to the theoretical value of −58 mV pH^{-1} at 25 °C [43], indicating a reversible two-proton coupled with two-electron transfer during the electrochemical redox reaction process Eq. (1):

$$\mathrm{GOD-FAD} + 2e^- + 2H^+ \leftrightarrow \mathrm{GOD-FADH_2} \quad (1)$$

Electrocatalytic properties of GOD/chitosan/α-ZrP modified electrode and glucose detection

Fig. 6 demonstrates the CVs of the GOD/chitosan/α-ZrP composite modified electrode in the nitrogen- and air-saturated 0.1% HAc buffer solution at pH 5.5. A couple of well-defined redox peaks were observed in both air- and nitrogen-saturated buffer solutions. However, the cathodic peak current is higher and the anodic peak current is lower in the air-saturated solution as compared with the corresponding peaks in the nitrogen-saturated solution, indicating that the intercalated GOD in the GOD/chitosan/α-ZrP composite nicely catalyzed the oxygen reduction Eqs. (2) and (3). When glucose was added to this air-saturated HAc buffer solution, the cathodic peak current decreased due to the oxidation of glucose catalyzed by GOD Eq. (4). Based on the decrease of the electrocatalytic response to dissolved oxygen, this GOD/chitosan/α-ZrP modified electrode was applied as a glucose biosensor:

$$\mathrm{GOD-FAD} + 2e^- + 2H^+ \rightarrow \mathrm{GOD-FADH_2} \quad (2)$$

$$\mathrm{GOD-FADH_2} + O_2 \rightarrow \mathrm{GOD-FAD} + H_2O_2 \quad (3)$$

$$\mathrm{Glucose} + O_2 \xrightarrow{\mathrm{GOD}} \mathrm{gluconolactone} + H_2O_2. \quad (4)$$

Fig. 7 displays the amperometric response of the GOD/chitosan/α-ZrP ternary composite modified electrode to the successive additions of glucose in the air-saturated and stirred 0.1% HAc buffer solutions (pH 5.5) at −435 mV. Each successive addition of glucose caused a decrease in the steady-state current. The linear calibration range for glucose is 0.25–8.0 mM (R = 0.9994, n = 14),

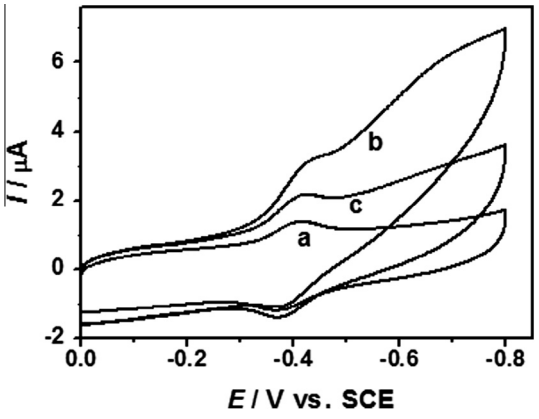

Fig.6. CVs of a GOD/chitosan/α-ZrP composite modified electrode in nitrogen-saturated (a), air-saturated (b), and air-saturated with 5 mM glucose (c) 0.1% HAc buffer solution at pH 5.5.

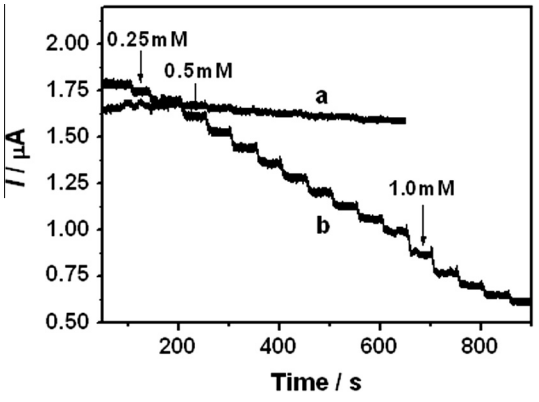

Fig.7. Amperometric response of a GOD/α-ZrP (a) and GOD/chitosan/α-ZrP (b) composite modified electrode in 0.1% HAc buffer solutions (pH 5.5) after the successive addition of glucose.

Table 1
Comparison of analytical parameters of GOD/chitosan/α-ZrP electrode with some other glucose biosensors.

Structure of biosensor	Linear range (mM)	Detection limit (mM)	Detection potential (V)	Reference
GOD/CNTs/chitosan/GCE	0–7.8	–	+0.4	[35]
MSCF/GOD/Nafion/GCE	0.05–5	0.034	−0.4	[36]
GOD/{PDDA/MnO_2}/graphite electrode	0.02–2.8	0.0098	–	[40]
AuNPs–GOD–MWCNTs–PVA/GCE	0.5–8	0.2	−0.4	[41]
GOD/ZnO/GOD/MWCNTs/GCE	0.00667–1.29	0.00222	−0.3	[42]
GOD–PEI–PGE	0.5–8.9	0.05	–	[44]
PDDA–GOD/Au/MWCNTs/GCE	0.5–5	–	−0.3	[45]
GOD/chitosan/α-ZrP/GCE	0.25∼8.0	0.076	−0.435	This work

Note: CNTs, carbon nanotubes; MSCF, mesocellular silica–carbon nanocomposite foam; PDDA, poly(diallyldimethylammonium); MnO_2, manganese dioxide; AuNPs, gold nanoparticles; MWCNTs, multiwalled carbon nanotubes; PVA, polyvinyl alcohol; ZnO, zinc oxide; PEI, polyethylenimine; PGE, polyethylene glycol; Au, gold.

with a detection limit of 0.076 mM. However, for the GOD/α-ZrP binary composite modified electrode, the steady-state current was almost unchanged along the successive addition of glucose. The phenomenon accords well with the result obtained by CD and UV characterizations, indicating the remarkable loss of enzymatic activity of the intercalated GOD in the GOD/α-ZrP binary composite. The reason may be due to the intensity interaction between GOD and α-ZrP leading to the denaturation of secondary formation of protein. As for the GOD/chitosan/α-ZrP ternary composite, the presence of the co-intercalated chitosan expanded the interlayer distance of α-ZrP to facilitate GOD intercalating. The intercalation of GOD into α-ZrP on a suitable interlayer space caused the recovery of the activity of GOD. Table 1 gives a comparison of analytical parameters of the GOD/chitosan/α-ZrP /GCE electrode with some other glucose biosensors. It was found that the linear range of this electrode is comparable to GOD immobilized in gold nanoparticles/carbon nanotubes/polyvinyl alcohol, carbon nanotubes/gold colloid/poly(diallyldimethyl–ammonium chloride composite, and polyethylenimine film, but is not as good as GOD immobilized in carbon nanotubes/chitosan and mesocellular silica–carbon nanocomposite foam/Nafion composite film.

For the electrochemical determination of glucose, the interferences of some electroactive species that coexist with glucose in human serum must be considered. In an air-saturated and stirred 0.1% HAc buffer solution (pH 5.5) containing 1.0 mM glucose, the response arising from 0.15 mM ascorbic acid (AA), 0.5 mM urea, and 0.125 mM uric acid (UA) is negligible.

The application of this GOD/chitosan/α-ZrP modified electrode for biological sample estimation of glucose was explored. For a human serum sample of diabetics, the glucose level was determined by cyclic voltammetry and the results are shown in Table 2 and Fig. S3 of the supplementary material.

In summary, a GOD/chitosan/α-ZrP ternary composite was prepared by co-intercalating GOD and chitosan into the interlayers of α-ZrP. The good performances—including the fast and direct electron transfer of GOD, the good electrocatalytic response to dissolved oxygen, and the detection of glucose in real biological samples—indicated that this GOD/chitosan/α-ZrP ternary composite may be a promising candidate for constructing the third-generation glucose biosensor. To improve the application of this GOD/chitosan/α-ZrP electrode on human serum samples without diabetics, the influence of co-intercalated chitosan amount on the detection limit and linear range should be investigated in the future.

Table 2
Glucose levels of human serum samples of diabetics estimated by GOD/chitosan/α-ZrP modified electrode.

Sample number	Detected value by this method (mM)	Detected value by hospital (mM)	Relative error (%)
1	18.80	18.28	2.85
2	19.38		6.02
3	15.74		−13.9
Average	17.97		1.68

Acknowledgments

This work was supported financially by the National Natural Science Foundation of China (21265008), the Natural Science Foundation of Jiangxi Province (20114BAB203011), and the Natural Science Foundation of the Department of Education of Jiangxi Province (GJJ11536).

Appendix A. Supplementary data

Supplementary data associated with this article can be found, in the online version, at http://dx.doi.org/10.1016/j.ab.2013.10.005.

References

[1] E. Ruiz-Hitzky, M. Darder, P. Aranda, Functional biopolymer nanocomposites based on layered solids, J. Mater. Chem. 15 (2005) 3650–3662.
[2] Q. Wang, Q. Gao, J. Shi, Enhanced catalytic activity of hemoglobin in organic solvents by layered titanate immobilization, J. Am. Chem. Soc. 126 (2004) 14346–14347.
[3] E. Serefoglou, K. Litina, D. Gournis, E. Kalogeris, A.A. Tzialla, I.V. Pavlidis, H. Stamatis, E. Maccallini, M. Lubomska, P. Rudolf, Smectite clays as solid supports for immobilization of β-glucosidase: synthesis, characterization, and biochemical properties, Chem. Mater. 20 (2008) 4106–4115.
[4] C.V. Kumar, A. Chaudhari, Proteins immobilized at the galleries of layered α-zirconium phosphate: structure and activity studies, J. Am. Chem. Soc. 122 (2000) 830–837.
[5] A. Bhambhani, C.V. Kumar, Enzyme–inorganic nanoporous materials: stabilization of proteins intercalated in α-zirconium(IV) phosphate by a denaturant, Microporous Mesoporous Mater. 110 (2008) 517–527.
[6] M. Kikuchi, S. Itoh, S. Ichinose, K. Shinomiya, J. Tanaka, Self-organization mechanism in a bone-like hydroxyapatite/collagen nanocomposite synthesized in vitro and its biological reaction in vivo, Biomaterials 22 (2001) 1705–1711.
[7] A. Bigi, E. Boanini, S. Panzavolta, N. Roveri, K. Rubin, Bonelike apatite growth on hydroxyapatite–gelatin sponges from simulated body fluid, J. Biomed. Mater. Res. 59 (2002) 709–714.
[8] J.-H. Choy, J.-M. Oh, M. Park, K.-M. Sohn, J.-W. Kim, Inorganic–biomolecular hybrid nanomaterials as a genetic molecular code system, Adv. Mater. 16 (2004) 1181–1184.
[9] J.-H. Choy, S.-Y. Kwak, Y.-J. Jeong, J.-S. Park, Inorganic layered double hydroxides as nonviral vectors, Angew. Chem. Int. Ed. 39 (2000) 4041–4045.
[10] K. Kamada, T. Nakamura, S. Tsukahara, Photoswitching of enzyme activity of horseradish peroxidase intercalated into semiconducting layers, Chem. Mater. 23 (2011) 2968–2972.
[11] C.V. Kumar, A. Chaudhari, High temperature peroxidase activities of HRP and hemoglobin in the galleries of layered Zr(IV) phosphate, Chem. Commun. (2002) 2382–2383.
[12] L. Gorton, A. Lindgren, T. Larsson, F.D. Munteanu, T. Ruzgas, I. Gazaryan, Direct electron transfer between heme-containing enzymes and electrodes as basis for third generation biosensors, Anal. Chim. Acta 400 (1999) 91–108.
[13] A.L. Ghindilis, P. Atanasov, E. Wilkins, Enzyme-catalyzed direct electron transfer: fundamentals and analytical applications, Electroanalysis 9 (1997) 661–674.
[14] A. Heller, Electrical wiring of redox enzymes, Acc. Chem. Res. 23 (1990) 128–134.

[15] F.A. Armstrong, H.A.O. Hill, N.J. Walton, Direct electrochemistry of redox proteins, Acc. Chem. Res. 21 (1988) 407–413.
[16] X. Han, W. Huang, J. Jia, S. Dong, E. Wang, Direct electrochemistry of hemoglobin in egg–phosphatidylcholine films and its catalysis to H_2O_2, Biosens. Bioelectron. 17 (2002) 741–746.
[17] J.F. Rusling, A-E.F. Nassar, Enhanced electron transfer for myoglobin in surfactant films on electrodes, J. Am. Chem. Soc. 115 (1993) 11891–11897.
[18] Q. Lu, T. Zhou, S. Hu, Direct electrochemistry of hemoglobin in PHEA and its catalysis to H_2O_2, Biosens. Bioelectron. 22 (2007) 899–904.
[19] S. Cosnler, C. Innocent, Y. Jouanneau, Amperometric detection of nitrate via a nitrate reductase immobilized and electrically wired at the electrode surface, Anal. Chem. 66 (1994) 3198–3201.
[20] D.-W. Pang, K.-Y. Won, Direct electrochemistry and electrocatalysis of heme proteins entrapped in agarose hydrogel films in room-temperature ionic liquids, Langmuir 21 (2005) 9260–9266.
[21] O. Nadzhafova, M. Etienne, A. Walcarius, Direct electrochemistry of hemoglobin and glucose oxidase in electrodeposited sol–gel silica thin films on glassy carbon, Electrochem. Commun. 9 (2007) 1189–1195.
[22] Z. Dai, S. Liu, H. Ju, H. Chen, Direct electron transfer and enzymatic activity of hemoglobin in a hexagonal mesoporous silica matrix, Biosens. Bioelectron. 19 (2004) 861–867.
[23] J.-J. Feng, J.-J. Xu, H.-Y. Chen, Direct electron transfer and electrocatalysis of hemoglobin adsorbed onto electrodeposited mesoporous tungsten oxide, Electrochem. Commun. 8 (2006) 77–82.
[24] E. Topoglidis, A.E.G. Cass, B. O'Regan, J.R. Durrant, Immobilisation and bioelectrochemistry of proteins on nanoporous TiO_2 and ZnO films, J. Electroanal. Chem. 517 (2001) 20–27.
[25] Y. Xian, Y. Xian, L. Zhou, F. Wu, Y. Ling, L. Jin, Encapsulation hemoglobin in ordered mesoporous silicas: influence factors for immobilization and bioelectrochemistry, Electrochem. Commun. 9 (2007) 142–148.
[26] L. Zhang, Q. Zhang, J. Li, Layered titanate nanosheets intercalated with myoglobin for direct electrochemistry, Adv. Funct. Mater. 17 (2007) 1958–1965.
[27] Y. Liu, C. Lu, W. Hou, J.-J. Zhu, Direct electron transfer of hemoglobin in layered α-zirconium phosphate with a high thermal stability, Anal. Biochem. 375 (2008) 27–34.
[28] L. Gao, Q. Gao, Hemoglobin niobate composite based biosensor for efficient determination of hydrogen peroxide in a broad pH range, Biosens. Bioelectron. 22 (2007) 1454–1460.
[29] X. Chen, C. Fu, Y. Wang, W. Yang, D.G. Evans, Direct electrochemistry and electrocatalysis based on a film of horseradish peroxidase intercalated into Ni–Al layered double hydroxide nanosheets, Biosens. Bioelectron. 24 (2008) 356–361.
[30] A. Bhambhani, C.V. Kumar, Protein/DNA/inorganic materials: DNA binding to layered α-zirconium phosphate enhances bound protein structure and activity, Adv. Mater. 18 (2006) 939–942.
[31] S.C. Holmström, A.J. Patil, M. Butler, S. Mann, Influence of polymer co-intercalation on guest release from aminopropyl-functionalized magnesium phyllosilicate mesolamellar nanocomposites, J. Mater. Chem. 17 (2007) 3894–3900.
[32] L. Liu, H.-T. Zhang, B. Shen, W. He, Y. Liu, G.-Y. Lu, J.-J. Zhu, PH-induced fabrication of DNA/chitosan/α-ZrP nanocomposite and DNA release, Nanotechnology 21 (2010) 105102.
[33] A. Heller, B. Feldman, Electrochemical glucose sensors and their applications in diabetes management, Chem. Rev. 108 (2008) 2482–2505.
[34] S. Liu, H. Ju, Reagentless glucose biosensor based on direct electron transfer of glucose oxidase immobilized on colloidal gold modified carbon paste electrode, Biosens. Bioelectron. 19 (2003) 177–183.
[35] Y. Liu, M. Wang, F. Zhao, Z. Xu, S. Dong, The direct electron transfer of glucose oxidase and glucose biosensor based on carbon nanotubes/chitosan matrix, Biosens. Bioelectron. 21 (2005) 984–988.
[36] S. Wu, H. Ju, Y. Liu, Conductive mesocellular silica–carbon nanocomposite foams for immobilization, direct electrochemistry, and biosensing of proteins, Adv. Funct. Mater. 17 (2007) 585–592.
[37] A.J. Patil, E. Muthusamy, S. Mann, Fabrication of functional protein–organoclay lamellar nanocomposites by biomolecule-induced assembly of exfoliated aminopropyl-functionalized magnesium phyllosilicates, J. Mater. Chem. 15 (2005) 3838–3843.
[38] M. Darder, M. Colilla, E. Ruiz-Hitzky, Biopolymer–clay nanocomposites based on chitosan intercalated in montmorillonite, Chem. Mater. 15 (2003) 3774–3780.
[39] E. Laviron, General expression of the linear potential sweep voltammogram in the case of diffusionless electrochemical systems, J. Electroanal. Chem. 101 (1979) 19–28.
[40] J.-J. Xu, J.-J. Feng, X. Zhong, H.-Y. Chen, Low-potential detection of glucose with a biosensor based on the immobilization of glucose oxidase on polymer/manganese oxide layered nanocomposite, Electroanalysis 20 (2008) 507–512.
[41] H. Zhang, Z. Meng, Q. Wang, J. Zheng, A novel glucose biosensor based on direct electrochemistry of glucose oxidase incorporated in biomediated gold nanoparticles–carbon nanotubes composite film, Sens. Actuators B 158 (2011) 23–27.
[42] F. Hu, S. Chen, C. Wang, R. Yuan, Y. Chai, Y. Xiang, C. Wang, ZnO nanoparticle and multiwalled carbon nanotubes for glucose oxidase direct electron transfer and electrocatalytic activity investigation, J. Mol. Catal. B 72 (2011) 298–304.
[43] A.-E.F. Nassar, Z. Zhang, N. Hu, J.F. Rusling, T.F. Kumosinski, Proton-coupled electron transfer from electrodes to myoglobin in ordered biomembrane-like films, J. Phys. Chem. B 101 (1997) 2224–2231.
[44] W. Zhang, Y. Huang, H. Dai, X. Wang, C. Fan, G. Li, Tuning the redox and enzymatic activity of glucose oxidase in layered organic films and its application in glucose biosensors, Anal. Biochem. 329 (2004) 85–90.
[45] Y.-L. Yao, K.-K. Shiu, Direct electrochemistry of glucose oxidase at carbon nanotube–gold colloid modified electrode with poly(diallyldimethylammonium chloride) coating, Electroanalysis 20 (2008) 1542–1548.